CALCULATION OF ANTENNA PERFORMANCE USING A HYBRID TECHNIQUE WHICH COMBINES THE MOMENT METHOD WITH AN ASYMPTOTIC CURRENT

Prof. Li Shi-zhi
Beijing Institute of Technology
Beijing, China

and

Gary A. Thiele
F.M. Tait Professor of Electrical Engineering
University of Dayton
Dayton, Ohio 45469-0227

ABSTRACT

Previously, this hybrid technique, a hybrid theory of diffraction, which combines the moment method with an asymptotic current, was used by Kim and Thiele to solve several 2-dimensional and 3-dimensional scattering problems when the incident field was a plane wave. In this paper the method is extended to problems in which the incident field is the near field of an antenna and also extended to calculate antenna impedance. As a sample problem, a monopole at the center of a circular disk is considered. Since the general procedure is an iterative one, the starting point in this problem is the assumption of the current distribution on the monopole. This current distribution generates the initial incident field which is turn gives the initial value of the asymptotic current on the circular disk (which is similar to the geometrical optics current).

The current in the asymptotic region (i.e., away from the edge of the disk), which is dominated by the optics type current on the entire surface of the scatterer, is solved by an iterative method to give the approximate surface current using the magnetic field integral equation. The difference between the approximate and true surface currents is calculated from the moment method current, which exists near shadow boundaries and/or sharp discontinuities in geometry. That is, the moment method current induces a current in the asymptotic region which is the difference between the optics type current and the true current.

The impedance may be calculated by using the infinite ground plane value plus the change caused by the finite extent of the ground plane through the use of equivalent currents.

Results are shown for both the impedance and the radiation patterns. These results are compared with other known results and the agreement is seen to be very good for both large (e.g., $ka > 6$) and small (e.g., $ka < 3$) ground planes.

I. INTRODUCTION

In this paper a hybrid technique is presented which combines the moment method with an asymptotic (AS) or optics (op) type current. This technique is called the hybrid theory of diffraction or HTD. The technique can be applied to consider the problem of a monopole located at the center of a circular disk. Here, the moment method is used to treat the current near discontinuities where the current is quite different from $2\hat{n} \times \overline{H}^i$, as indicated by Fig. 1, while in other regions the current is determined from an asymptotic evaluation of the H-field integral equation.

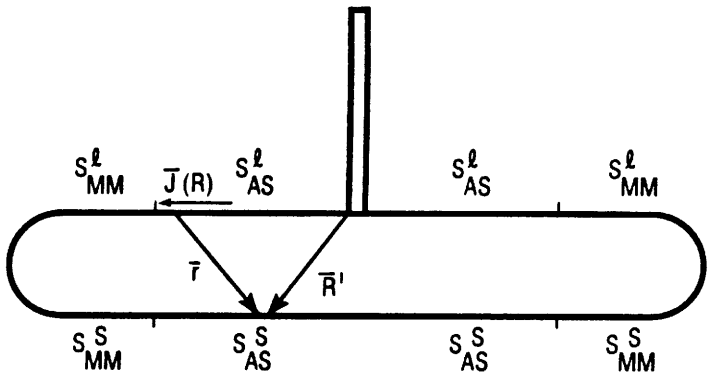

Figure 1 - The surface of the disk is divided into four regions.

In the actual problem considered here, the quarter wave monopole is vertically located at the center of a circular disk. The disk is assumed to be perfectly conducting, of radius a and with the thickness d = 0.10λ. The antenna lies along the axis perpendicular to the disk with its lower end in contact with the voltage source on the disk. The radius is equal to 0.003λ.

First we use the moment method to get the current distribution on the monopole on an infinite ground plane, then use the monopole's near zone field expression to get the incident magnetic field $\overline{H}^i$ on the surface of the disk. Here, the geometrical optics type current, $2\hat{n} \times \overline{H}^i$ is a starting point in an integral equation/iteration procedure, to obtain the current on the surface of the disk.

According to the Equivalence Theorem, the far field of this system may be calculated directly by using the monopole current and the currents on both sides of the disk.

The impedance may be calculated by using the infinite ground plane value plus the change caused by the finite extent of the ground plane. Two general advantages of this method are that it can analyze problems larger than can normally be handled by the moment method alone, and that it can treat problems for which the required diffraction coefficients are not known.

II. CURRENT DISTRIBUTION ON THE CIRCULAR DISK

The central part of this problem consists of using the HTD to get the current distribution on the disk. The current distribution on the circular disk is initially excited by the current on the monopole.

A. General Equations

We will use the following form of the magnetic field integral equation [1,2] to determine the general equation for the hybrid theory of diffraction.

$$\overline{J}(\overline{R}) = T\hat{n} \times \overline{H}^{i}(\overline{R}) + T\hat{n} \times \int_{s} \overline{J}(\overline{R}') \times \nabla' G(r)\, ds' \tag{1}$$

where

$$T = (1-\Omega/4\pi)^{-1}$$

Here Ω is a solid angle with respect to the point P, and we use the T factor to solve the singularity problem which will be discussed later. The vectors $\overline{R}$ and $\overline{R}'$ are the position vectors of the observations point P and the source point P′, respectively, and $r = |\overline{R}' - \overline{R}|$ is the distance between the points P and P′ as shown in Fig. 2. The unit vector $\hat{n}$ is outward and normal to the surface at P. $\overline{H}^{i}(\overline{R})$ is the incident magnetic field at point P on the surface. The symbol $\int$ represents the principle value of integration. The free space Green's function G(r) is:

$$G(r) = \frac{e^{-jkr}}{4\pi r} \tag{2}$$

where k is the free space propagation constant.

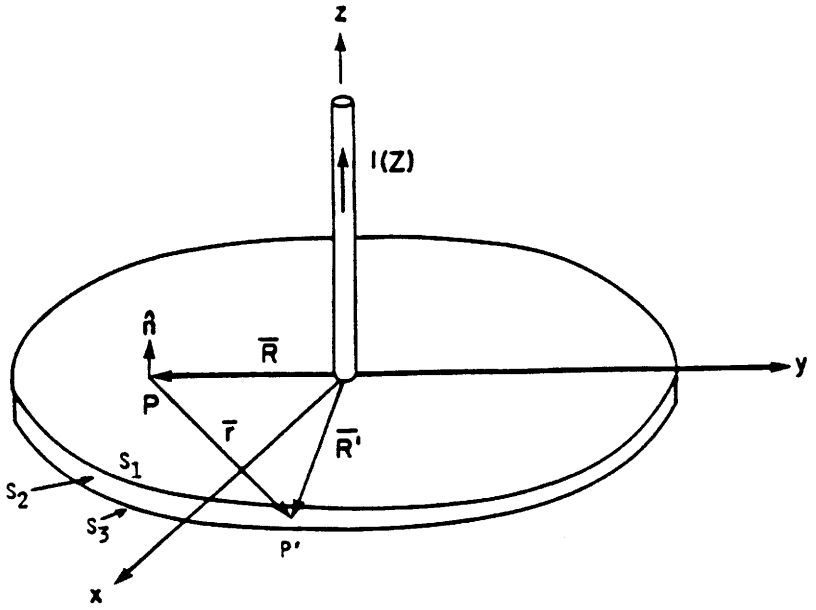

Figure 2 - Monopole at the center of the disk.

The development of the general equations proceeds as given by Kim and Thiele in [1] and need not be repeated here. In this paper we prefer to dwell on the specialization of the general equations (12) - (32) in Kim and Thiele to a problem where the source is on the scattering body (i.e., monopole on a disk) rather than when the source is far from the scatterer.

B. Monopole Located at the Center of the Disk

Now consider the situation of a monopole which is located at the center of a disk. The system is symmetrical to the monopole's axis and also there is a symmetrical current distribution on the surface of the disk. Obviously the direction of the current on the disk surface is along the radius of the disk.

To solve for the current induced by the monopole, the magnetic field integral equation can be applied as in [1]. Thus, for the first order approximation we have, similar to (11-13) in [1]:

$$\bar{J}^1_{op}(\bar{R}) = T\hat{n}_1 \times \bar{H}_i(\bar{R}) \tag{3}$$

$$\bar{J}^2_{op}(\bar{R}) = T\hat{n}_2 \times \bar{H}_i(\bar{R}) + T\hat{n}_2 \times \sum_{\substack{K=1 \\ K\neq 2}}^{3} \int_{S^K} \bar{J}^K_{op}(\bar{R}') \times \nabla' G(r)\, ds' \tag{4}$$

$$\bar{J}^3_{op}(\bar{R}) = T\hat{n}_3 \times \bar{H}_i(\bar{R}) + T\hat{n}_3 \times \sum_{k=1}^{2} \int_{S^K} \bar{J}^K_{op}(\bar{R}') \times \nabla' G(r)\, ds' \tag{5}$$

where $\hat{n}_1$, $\hat{n}_2$ and $\hat{n}_3$ are the outward normal vectors to the surface s^1, s^2 and s^3 respectively as identified in Fig. 2. Surface s^1 is the lit surface while surfaces s^2 and s^3 are shadowed. For conceptual reasons we will sometimes refer to s^1 as s^l and to either s^2 and s^3 as s^s (see Fig. 1).

The first order approximate current in the moment method (MM) regions (see Fig. 2) can be obtained from:

$$\bar{I}^1_{MM}(\bar{R}) = T\hat{n}_1 \times \sum_{K=2}^{3} \int_{S^K_{MM}} \bar{I}^K_{MM}(\bar{R}') \times \nabla' G(R)\, ds'$$

$$+ T\hat{n}_1 \times \sum_{K=2}^{3} \int_{S^k} \bar{J}^K_{op}(\bar{R}') \times \nabla' G(r)\, ds' \tag{6}$$

$$\bar{I}^2_{MM}(\bar{R}) = T\hat{n}_2 \times \sum_{K=1}^{3} \int_{S^K_{MM}} \bar{I}^K_{MM}(\bar{R}') \times \nabla' G(r)\, ds' \tag{7}$$

$$\bar{I}^3_{MM}(\bar{R}) = T\hat{n}_3 \times \sum_{K=1}^{2} \int_{S^K_{MM}} \bar{I}^K_{MM}(\bar{R}') \times \nabla' G(r)\, ds' \tag{8}$$

which are similar to (29) and (30) in [1]. The expressions for the currents in the asymptotic regions (AS) are the same as Equations (6) to (8) except that the observation points are moved from the MM-region to the AS-regions as in (31) and (32) in [1].

C. Moment Method Current

The moment method is used to solve Equations (6) to (8). For this purpose we use simple pulse basis functions and the point-matching technique. As we expect from the equations we derived, the resulting impedance matrix will be a little complicated because there are three unknown currents involved in the calculations. Therefore, we will obtain an approximate expression for the matrix by ignoring certain terms in the equations.

Now considering the observation points are limited to the moment method region and that the current in the nearest region to the observation points will most contribute to the current at the observations points, we can ignore the current terms containing $\bar{I}^l_{AS}(\bar{R}')$ or $\bar{I}^s_{AS}(\bar{R}')$ in equations (27) and (28) of Reference 1 to derive the first order approximations for $\bar{I}^l_{MM}(\bar{R})$ and $\bar{I}^s_{MM}(\bar{R})$. Therefore, we have:

$$\overline{I}^1_{MM}(\overline{R}) = T\hat{n}_1 \times \int_{S^2_{MM}} \overline{I}^2_{MM} \times \nabla' G(R, R'_2)\, ds_2 + T\hat{n}_1 \times \int_{S^3_{MM}} \overline{I}^3_{MM} \times \nabla' G(R, R'_3)\, ds_3$$

$$+ T\hat{n}_1 \times \sum_{k=2}^{3} \int_{S^K} \overline{J}^K_{op}(\overline{R}'_k) \times \nabla' G(R, R'_K)\, ds_K \tag{9}$$

$$\overline{I}^2_{MM}(\overline{R}'_2) = T\hat{n}_2 \times \int_{S^1_{MM}} I^1_{MM}(\overline{R}) \times \nabla' G(R'_2, R')\, ds_1 \tag{10}$$

$$\overline{I}^3_{MM}(\overline{R}'_3) = T\hat{n}_3 \times \int_{S^1_{MM}} \overline{I}^1_{MM}(\overline{R}) \times \nabla' G(R'_3, R')\, ds_1 \tag{11}$$

Substituting Equations (10) and (11) into Equation (9),

$$\overline{I}^1_{MM}(\overline{R}) - T\hat{n}_1 \times \left\{ \int_{S^2_{MM}} \left[T\hat{n}_2 \times \int_{S^1_{MM}} \overline{I}^1_{MM}(\overline{R}') \times \nabla' G(R'_2, R')\, ds_1 \right] \times \nabla' G(R, R'_2)\, ds_2 \right\}$$

$$- T\hat{n}_1 \times \left\{ \int_{S^3_{MM}} \left[T\hat{n}_3 \times \int_{S^1_{MM}} \overline{I}^1_{MM}(\overline{R}') \times \nabla' G(R'_3, R)\, ds_1 \right] \times \nabla' G(R, R'_3)\, ds_3 \right\}$$

$$= T\hat{n}_1 \times \sum_{K=2}^{3} \int_{S^K} \overline{J}^K_{op}(\overline{R}'_K) \times \nabla' G(R, R'_K)\, ds' \tag{12}$$

Taking

$$\overline{I}^1_{MM}(\overline{R}) = \sum_{n=1}^{N} \overline{I}_n P(\overline{R} - \overline{R}_n) \tag{13}$$

where

$$P(\overline{R}) = \begin{cases} 1 \text{ for } |\overline{R} - \overline{R}_n| < \dfrac{\Delta P}{2} \\ 0 \text{ elsewhere} \end{cases} \tag{14}$$

$\Delta P = \dfrac{\omega_{ck}}{N_K}$, N_K is the number of subintervals in ω_{ck}

then

$$\sum_{n=1}^{N} \bar{I}_n P(\bar{R}-\bar{R}_n) - T\hat{n}_1 \times \left\{ \int_{S_{MM}^2} \left[T\hat{n}_2 \times \int_{S_{MM}^1} \sum_{n=1}^{N} \bar{I}_n P(\bar{R}-\bar{R}_n) \times \nabla' G(R_2', R)\, ds_1 \right] \times \nabla' G(R, R_2')\, ds_2 \right\}$$

$$- T\hat{n}_1 \times \left\{ \int_{S_{MM}^3} \left[T\hat{n}_3 \times \int_{S_{MM}^1} \sum_{n=1}^{N} \bar{I}_n P(\bar{R}-\bar{R}_n) \times \nabla' G(R_3', R')\, ds_1 \right] \times \nabla' G(R, R_3')\, ds_3 \right\}$$

$$= T\hat{n}_1 \times \sum_{k=2}^{3} \int_{S^K} \bar{J}_{op}^{K} (\bar{R}_K') \times \nabla' G(R, R_K)\, ds' \qquad (15)$$

Multiplying both sides of Equation (15) by $\delta(\bar{R} - \bar{R}_M)$, $m = 1, 2, 3, \ldots N$, integrating them over the surface s^1_{MM} and dividing both sides by Δs, then we have:

$$\sum_{n=1} \bar{I}_n P(\bar{R}_m-\bar{R}_n) - 2\hat{n}_1 \times \left(\int_{S_{mm}^2} T\hat{n}_2 \times \left[\int_{S_{MM}^1} \sum_{n=1}^{N} \bar{I}_n P(\bar{R}_M-\bar{R}_n) \times \nabla' G(R_2', R)\, ds_1 \right] \right.$$

$$\times \nabla' G(R_n, R_2')\, ds_2 + \int_{S_{MM}^3} \left\{ 2\hat{n}_3 \times \left[\int_{S_{MM}^1} \sum_{n=1}^{N} \bar{I}_N P(\bar{R}_m-\bar{R}_n) \times \nabla' G(R_3', R')\, ds_1 \right] \right\}$$

$$\left. \times \nabla' G(R_m, R_s')\, ds_3 \right) = T\hat{n}_1 \times \sum_{K=2}^{3} \int_{S^K} \bar{J}_{op}^{k} (\bar{R}_K) \times \nabla' G(R_m, R_K')\, ds' \qquad (16)$$

We could also use the generalized impedance matrix representation:

$$[Z_{mn}]\,[I_N] = [V_m], \qquad m, n, = 1, 2, 3, \ldots N \qquad (17)$$

where the elements of the impedance matrix $[Z_{mn}]$ are:

$$Z_{mn} = P(\bar{R}_M-\bar{R}_n) - 2\hat{n}_1 \times \int_{S_{MM}^2} \left\{ T\hat{n}_2 \times \left[\hat{J}_n \times \nabla' G(R_2', R_n') \right] \right\} \times \nabla' G(R_m, R_2')\, ds_2$$

$$+ \int_{S_{MM}^3} \left\{ 2\hat{n}_3 \times \left[\hat{J}_n \times \nabla' G(R_3', R_n') \right] \right\} \times \nabla' G(R_m, R_s')\, ds_3\, \Delta s \qquad (18)$$

where $| \hat{J}_n | = 1$.

D. The Additional Asymptotic Currents $\overline{I}^{t}_{AS}(\overline{R})$ and $\overline{I}^{t}_{AS}(\overline{R})$

By the same procedure, we can derive integral equations for $\overline{I}^{t}_{AS}(\overline{R})$ and $\overline{I}^{s}_{AS}(\overline{R})$. However, we can write down directly those equations by noting that the additional current in the asymptotic regions also satisfy Equations (6), (7), and (8) for their first approximations. Thus, we can write the following equations for $\overline{I}^{t}_{AS}(\overline{R})$, (i.e. $\overline{I}^{1}_{AS}$) and $\overline{I}^{s}_{AS}(\overline{R})$, (i.e. $\overline{I}^{2}_{AS}$ and $\overline{I}^{3}_{AS}$):

$$\overline{I}^{1}_{AS}=2\hat{n}_1\times\sum_{K=2}^{3}\int_{S_K}\overline{J}^{K}_{op}(\overline{R'})\times\nabla' G(r)\,ds'_k+2\hat{n}_1\times\sum_{K=2}^{3}\int_{S_K}\overline{I}^{K}_{MM}(\overline{R'})\times\nabla' G(r)\,ds'_k \tag{19}$$

$$\overline{I}^{2}_{AS}=T\hat{n}_2\times\int_{S_{MM}^{t}}\overline{I}^{t}_{AS}(\overline{R})\times\nabla' G(r)\,ds'_t+T\hat{n}_2\times\sum_{K=2}^{3}\int_{S_{MM}^{K}}\overline{I}^{K}_{MM}(\overline{R'})\times\nabla' G(r)\,ds'_k \tag{20}$$

$$\overline{I}^{3}_{AS}=2\hat{n}_3\times\int_{S_{MM}^{t}}\overline{I}^{t}_{AS}(\overline{R})\times\nabla' G(r)\,ds'_t+2\hat{n}_3\times\int_{S_{MM}^{2}}\overline{I}^{2}_{AS}(\overline{R})\times\nabla' G(r)\,ds'_2 \tag{21}$$

E. The Higher Order Approximation and Total Current

We can obtain the higher order approximation for $I^{t}_{MM}(R)$ and $I^{S}_{MM}(R)$ by substituting Equations (9) to (11) and Equations (19) to (21) into Equations (6), (7), and (8) which are given by:

$$\overline{I}^{1}(\overline{R})=2\hat{n}_1\times\int\overline{I}^{2}(\overline{R'})\times\nabla' G(r)\,ds'+2\hat{n}_1\times\int\overline{I}^{3}(\overline{R'})\times\nabla' G(r)\,ds'$$
$$+2\hat{n}_1\times\sum_{K=2}^{3}\int_{S_K}\overline{J}^{K}_{op}(R)\times\nabla' G(r)\,ds'_k \tag{22}$$

$$\overline{I^{2}}(\overline{R}) = T\hat{n}_2\times\int\overline{I}^{1}(\overline{R'})\times\nabla' G(r)\,ds'+T\hat{n}_2\times\int\overline{I}^{3}(\overline{R'})\times\nabla' G(r)\,ds' \tag{23}$$

$$\overline{I}^{3}(\overline{R})=2\hat{n}_3\times\int\overline{I}^{1}(\overline{R'})\times\nabla' G(r)\,ds'+2\hat{n}_3\times\int\overline{I}^{2}(\overline{R'})\times\nabla' G(r)\,ds \tag{24}$$

The total current can then be obtained as follows:

$$\overline{J}^{1}(\overline{R}) = \overline{J}^{1}_{op}(\overline{R}) + \overline{I}^{1}(\overline{R}) \tag{25}$$

$$\overline{J}^{2}(\overline{R}) = \overline{J}^{2}_{op}(\overline{R}) + \overline{I}^{2}(\overline{R}) \tag{26}$$

$$\overline{J}^{3}(\overline{R}) = \overline{J}^{3}_{op}(\overline{R}) + \overline{I}^{3}(\overline{R}) \tag{27}$$

F. The Singularity Problem

The integral equation for the curved surface has as many singular points as observation points. We can solve this problem by using the T factor [3] in the magnetic field integral equation in Equation (1). The Ω represents the absolute value of solid angle subtended by s_2 at x in the limit as r vanishes (see Fig. 3).

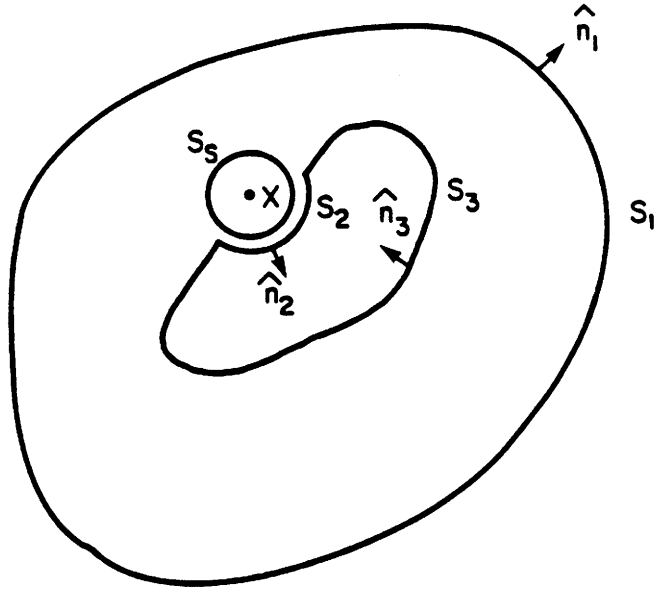

Figure 3 The mathematical surfaces in the integral equations for evaluating the singularity.

G. Numerical Results

Numerical results for ground planes of four different sizes are shown in Figures 4a-d. The sizes are ka = 3,4,5 and $(42)^{1/2}$ in Figures 4a-d respectively. Plotted are both the real part of the normalized currents and the imaginary part. Also given is the normalized magnitude I/I_o. From left to right, the abscissa represents the distance from the base of the quarter wave monopole at the center of the disk to the edge (i.e. o to a). The abscissa from a to o then gives the distance from the edge (of finite thickness) to the center of the disc on the bottom (shadowed) side. We observe that, while the current is smaller on the shadowed side, it is not negligibly small there.

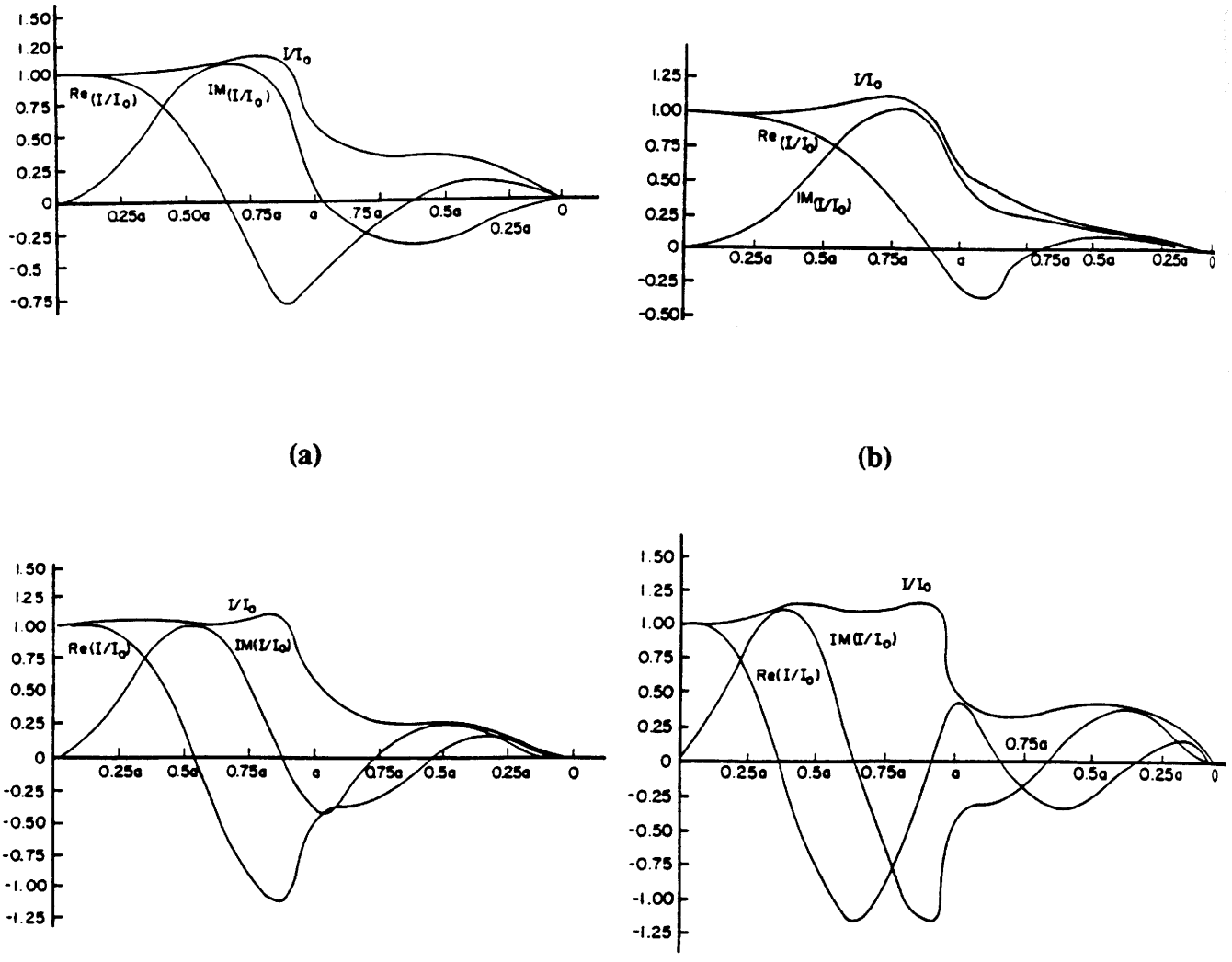

Figure 4(a-d) Ratio of radial current I (on both sides of the ground plane) to the amplitude I_o of the current on the antenna plotted against distance from the center for the cases when ka = 3,4,5, $(42)^{1/2}$.

In Figure 5 are plotted the four normalized current amplitudes but only on the illuminated side of the disks. When this figure is compared with the same data in [4] it is clear that the results here are in excellent agreement with those in [4]. In the next section we will also see that the radiation patterns computed from these currents are also in agreement with those in [4].

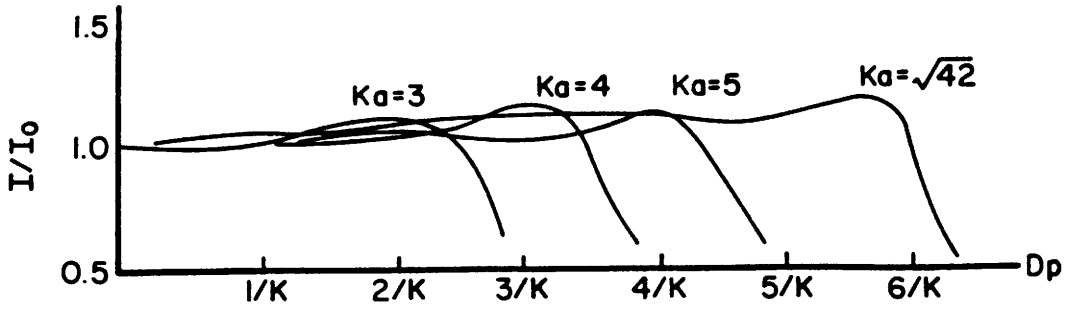

Figure 5 Absolute values of the ratio of radial current I (on the antenna side of the ground plane) to the amplitude I_o of the current on the antenna plotted to common scale against distance from the center of cases when ka = $3,4,5,(41)^{1/2}$.

III. RADIATION PATTERN

Let us consider the radiation pattern of the monopole which is mounted at the center of the disk as shown in Figure 6.

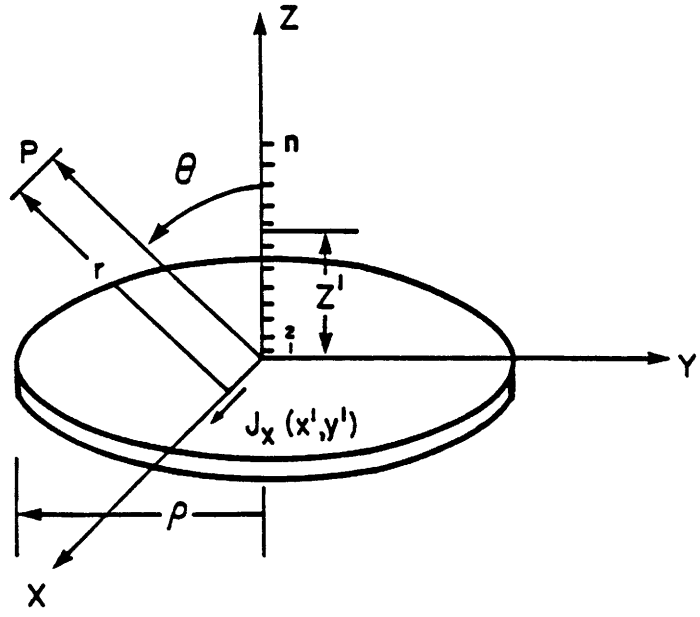

Figure 6 Geometry for far field calculations.

The field at large distance from the radiating system can be calculated from the current distribution on the monopole and the equivalent current distribution on both sides of the disk.

The total far field pattern can be evaluated by the superposition principle. For example, we divide the monopole into many segments. For the i^{th} segment the field E_i is evaluated from current $I_i(z)$, so the field of the monopole, $E^m(\theta)$, can be written as follows:

$$E^m(\theta) = \sum_{i=1}^{N} j\frac{\eta I_i}{2} sin\theta \left(\frac{e^{-jkr}}{r}\right) e^{jkz'\cos\theta} dz' \tag{28}$$

where

$\eta = 367.2727\ \Omega$

$k = \frac{2\pi}{\lambda}$

r = distance from origin to point p

θ = angle between z and r

The field $E_1^s(\theta)$ in the x-z plane is evaluated from the current distribution on the lit surface of the disk (see Fig. 6) as follows [5]:

$$E_1^s(\theta) = \underset{\substack{\text{lit}\\ \text{surface}}}{E(\theta)} = \frac{j\pi\mu\cos\theta}{2kr_1} e^{-jkr_1} \iint_{s_1} J_x(x', y')\, e^{jky'\sin\theta} ds' \tag{29}$$

x', y' are the coordinates of the current on the lit surface of the disk

s_1 is the lit surface of the disk

r_1 is the distance from the current on the lit surface to point p.

Similarly for the shadow side we have:

$$E_2^s(\theta) = \underset{\substack{\text{shadow}\\ \text{surface}}}{E(\theta)} = \frac{j\omega\mu\cos\theta}{2kr_2} e^{-jkr_2} \iint_{S_2+S_3} J_x(x', y')\, e^{-jky'\sin\theta} ds' \tag{30}$$

x', y' are the coordinates of the current on the shadow surface of the disk

s_2+s_3 is the shadow part surface of the disk

r_2 is the distance from the current on the shadow surface to point p

Thus, the total field, $E^T(\theta)$, of this radiating system is:

$$E^T(\theta) = E^m(\theta) + E_1^s(\theta) + E_2^s(\theta) \quad . \tag{31}$$

We see that the patterns for the parameter values ka = $3,4,5,(42)^{1/2}$ in Figs. 7a to 7d differ greatly from the pattern in Fig. 7e for the infinite ground plane case. The radiation field shows no sign of approaching the case corresponding to the isolated half-wave length antenna. While the isolated antenna radiates its energy most strongly in a direction perpendicular to the antenna, the finite ground plane system radiates preponderantly in an oblique direction.

In patterns in Figs. 7a to 7d, solid curves represent the results obtained using the wave function of an oblate spheroid [4] and the dotted curves are our results obtained by using the hybrid theory of diffraction.

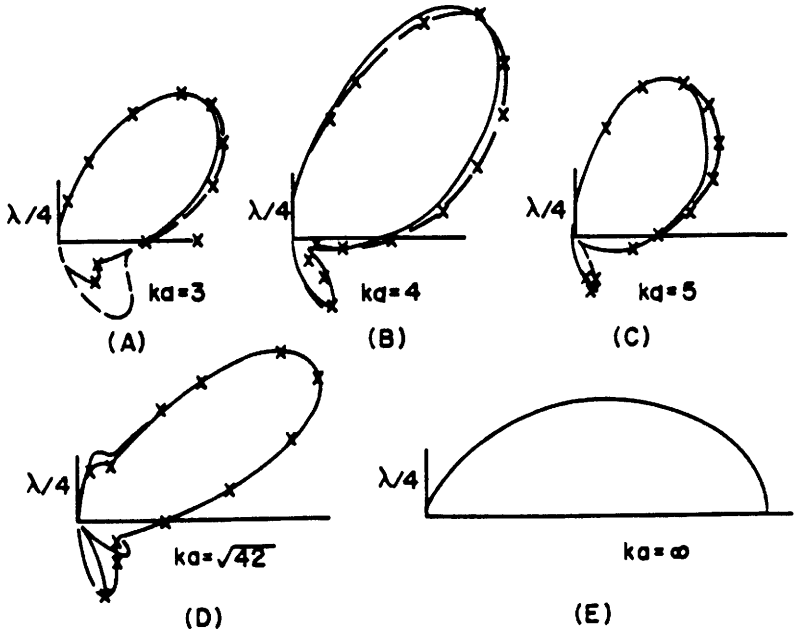

Figure 7(a-e) Linear field patterns (polar graphs in any elevation plane) of a quarter wavelength antenna situated on circular ground planes for the cases when ka = $4,3,5,(41)^{1/2}$, ∞
x_____x hybrid method
_____ classical method

IV. EXPRESSION FOR THE INPUT IMPEDANCE

The purpose of this section is to obtain an expression for the input impedance, Z, of the antenna as a function of the radius of the disk [6]. This is done by calculating the change in input impedance of the monopole on an infinite ground plane due to the finite extent of the actual ground plane. Image theroy is used where appropriate.

Let σ denote a surface which surrounds the antenna, such as indicated in Fig.8.

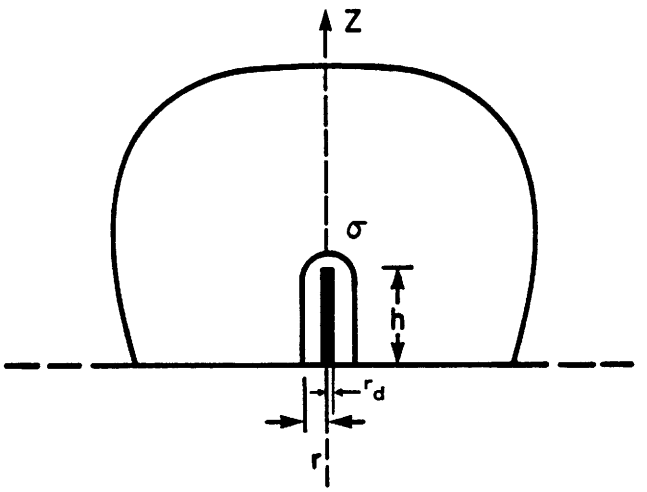

Figure 8 Surface for poynting vector ingetration.

By applying Poynting's theorem to this surface, one obtains the following results:

$$P=\frac{1}{2}\int_{\sigma}(\bar{E}x\overline{H^*})\cdot\hat{n}d\sigma \tag{32}$$

where the real part of P = average power being radiated by the antenna, the imaginary part of P = 2ω x difference between mean electric and magnetic energies inside σ, and $\hat{n}$ is the unit outward normal vector to σ.

We assume

$$\bar{E} = \bar{E}^{\infty} + \bar{E}^{s}$$

$$\bar{H} = \bar{H}^{\infty} + \bar{H}^{s} \tag{33}$$

$\bar{E}^{\infty}$ *and* $\bar{H}^{\infty}$ are the fields in the infinite ground plane situation. $\bar{E}^{s}$ *and* $\bar{H}^{s}$ are the diffraction fields because of the finite ground plane. So we have:

$$P = \frac{1}{2}\int_{\sigma}(\bar{E}^{\infty}+\bar{E}^{s})\ x\ (\bar{H}^{\infty}+\bar{H}^{s})^{*}\cdot\hat{n}ds \tag{34}$$

The fields, $\bar{E}^{\infty}+\bar{E}^{s}$, $\bar{H}^{\infty}+\bar{H}^{s}$, satisfy the Maxwell equations and correctly represent the power being radiated when the surface σ is a considerable distance from the antenna. Accordingly, these fields must also represent correctly the power being radiated if the surface σ is taken to be close to the antenna. In particular, if σ is allowed to shrink until it just surrounds the antenna, it is seen in our problem here that:

$$P = \lim_{r \to r_d} \frac{1}{2} \int_0^h \int_0^{2\pi} \left(E_z^{\infty}+E_x^{s}\right) \left(H_\phi^{\infty}+H_\phi^{s}\right)^* (\hat{z} \times \hat{\phi}) \cdot \hat{r}\, r\, d\phi\, dz$$

$$= - \lim_{r \to r_d} \frac{2\pi r}{2} \int_0^h \left(E_z^{\infty}+E_z^{s}\right) \left(H_\phi^{\infty}+H_\phi^{s}\right)^* dz \tag{35}$$

where r_d is the radius of the monopole.

The results of this section may also be obtained by taking σ to be a large spherical surface. This approach, however, involves more algebra than the one being used here.

The quantity P is related to the input impedance by:

$$P = \frac{1}{2} ZI(0)\, I^*(0) \tag{36}$$

I(0) is the current at the driving point of the antenna. Inserting this expression for P, Equation (36) may be written in the following form:

$$ZI(0) \times I^*(0) = - \lim_{r \to r_d} 2\pi r \left\{ \int_o^h \left(E_z^{\infty}+E_z^{s}\right) \left(H_\phi^{\infty}+H_\phi^{s}\right)^* dz \right\} \tag{37}$$

we know [6]

$$\lim_{r \to r_d} \left(H_\phi^{\infty}+H_\phi^{s}\right) = \lim_{r \to r_d} H_\phi^{\infty} = \lim_{r \to r_d} \frac{I(z)}{2\pi r}, 0 \le z \le h \tag{38}$$

H_ϕ^s does not contribute to this expression, since changes in radial current on the ground screen (represented by H_ϕ^s) do not affect the distribution of current along the vertical antenna. This can readily be shown from the integral representation [6] for H_ϕ^s.

Hence, it follows that:

$$ZI(0)\, I^*(0) = - \int_0^h \left[E_z^{\infty}+E_z^{s}\right]_{r_d} I^*(z)\, dz \tag{39}$$

Let Z_o denote the impedance of the antenna over an infinite screen. Directly from the definition of E_z^2, $E_z^s=0$ in the infinite ground screen case. Thus,

$$Z_o I(0)\, I^*(0) = - \int_0^h E_z^{\infty}\big|_{r_d} I^*(z)\, dz \tag{40}$$

Therefore, the first integral appearing in Equation (39) is related to the impedance over an infinite screen. When this information is inverted, Equation (39) becomes:

$$(Z-Z_o)\,I(0)\,I^*(0) = -\int_0^h E_z^s|_{I_d} I^*(z)\,dz \tag{41}$$

Thus, it is seen that the effects of the infinite screen subtract out yielding an expression for the change of the impedance, $Z\text{-}Z_o$.

At this point we have the assumed current distribution on the monopole and induced distribution on the disk. Now we need the (new) $[E_z^s]$ along the monopole. From Equation (33) we have:

$$E_z^s = E_z^\infty - E_z \tag{42}$$

We can calculate E_z^∞ by using the image principle and the near-zone field of a sinusoidal line source as follows:

$$E_z^\infty = \frac{-j\eta I_o}{4\pi\sin(kh)}\left\{\frac{e^{-jkr_1}}{R_1} + \frac{e^{-jkr_2}}{R_2} - 2\cos(kh)\,\frac{e^{-jk\rho}}{\rho}\right\} \tag{43}$$

where I_o is the terminal current of a monopole on an infinite ground plane and R_1, R_2 are defined in Fig. 9. Also we can calculate E_z from the current distribution on the monopole and the current distribution on the disk [15]:

$$E_z = \frac{-j\eta I_o}{4\pi\sin(kh)}\left\{\frac{e^{-jkr_2}}{R_2} - \cos(kh)\,\frac{e^{-jk\rho}}{\rho}\right\}$$

$$+ \int \{-j\omega\mu\bar{J}(\bar{\rho}')\,G + \frac{1}{j\omega\epsilon}\bar{J}(\bar{\rho}')\cdot\nabla\nabla G\}\,ds \tag{44}$$

$\bar{J}(\bar{\rho}')$ = current density distribution on the surface of the disk shown in Fig. 10.

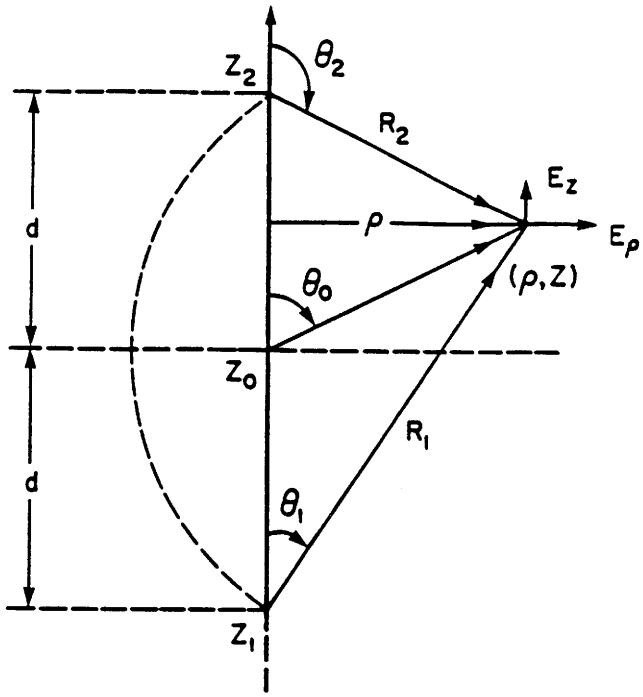

Figure 9 The near field of the dipole.

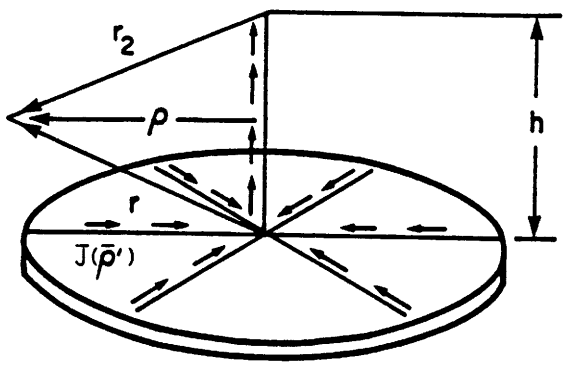

Figure 10 The near field of the monopole and the disk.

We assume the $I_{o\ \text{infinite ground plane}} \simeq I_{o\ \text{finite ground plane}}$, so from Eqs. (42) to (44) we have

$$E_z^s = E_z^{\infty} - E_z$$

$$E_z^s = \frac{\eta}{4\pi \sin(kh)} \left\{ \frac{e^{-jkr_1}}{r_1} - \cos(kh)\, \frac{e^{-jk\rho}}{\rho} \right\}$$

$$- \int_s \{ -j\omega\mu \bar{J}(\bar{\rho}')\, G + \frac{1}{j\omega\epsilon} \bar{J}(\bar{\rho}') \cdot \nabla\nabla G \}\, ds \qquad (45)$$

This field needs to be evaluated along the axis of the monopole. To save computation time we can use Eq. (45) to get the field at the edge of the disk, then use the equivalent magnetic current [7,8,9] to get the field along the axis of the monopole as shown in Fig. 11.

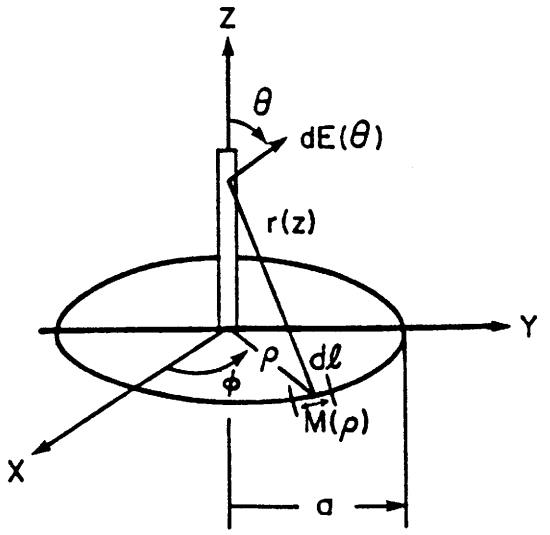

Figure 11 The equivalent magnetic current density.

We start with the equivalent magnetic current density:

$$\overline{M}(\rho) = \hat{n} \times E_z^s(\rho) \tag{46}$$

Now we should calculate the electric field along the monopole from the equivalent magnetic current density $\overline{M}(\rho)$. We know the electric field in a plane perpendicular to a magnetic current element $d\ell$ is given by [7,8,9] (see Fig 11):

$$d\overline{E}^{\theta} = \frac{Md\ell}{4\pi}\left(\frac{j\omega}{cr} + \frac{1}{r^2}\right) e^{-jkr} \tag{47}$$

So, upon integrating $d\overline{E}^{\theta}$, we can get $E_z^s|_{r_d}$ as:

$$\overline{E}_z^s|_{r_d} = \frac{M\rho^2}{2r}\left(\frac{jk}{r} + \frac{1}{r^2}\right) e^{-jkr} \tag{48}$$

Here $c = \frac{1}{\sqrt{\mu_o \epsilon_o}}$. Substituting Equation (48) into Equation (41) enables us to calculate the

change in antenna impedance.

The impedance of the monopole on an infinite plane Z_o can be calculated by the moment method. For example, $Z_o = 31.98 - j11.21$ when $h = 0.227\lambda$ and $r_d = 0.003\lambda$. From

$$Z - Z_o = \delta Z \tag{49}$$

we obtained

$$Z = Z_o + \delta Z \tag{50}$$

Figure 12 represents the result that we obtained by this method. The results compare well with other results in the literature [9,10,16].

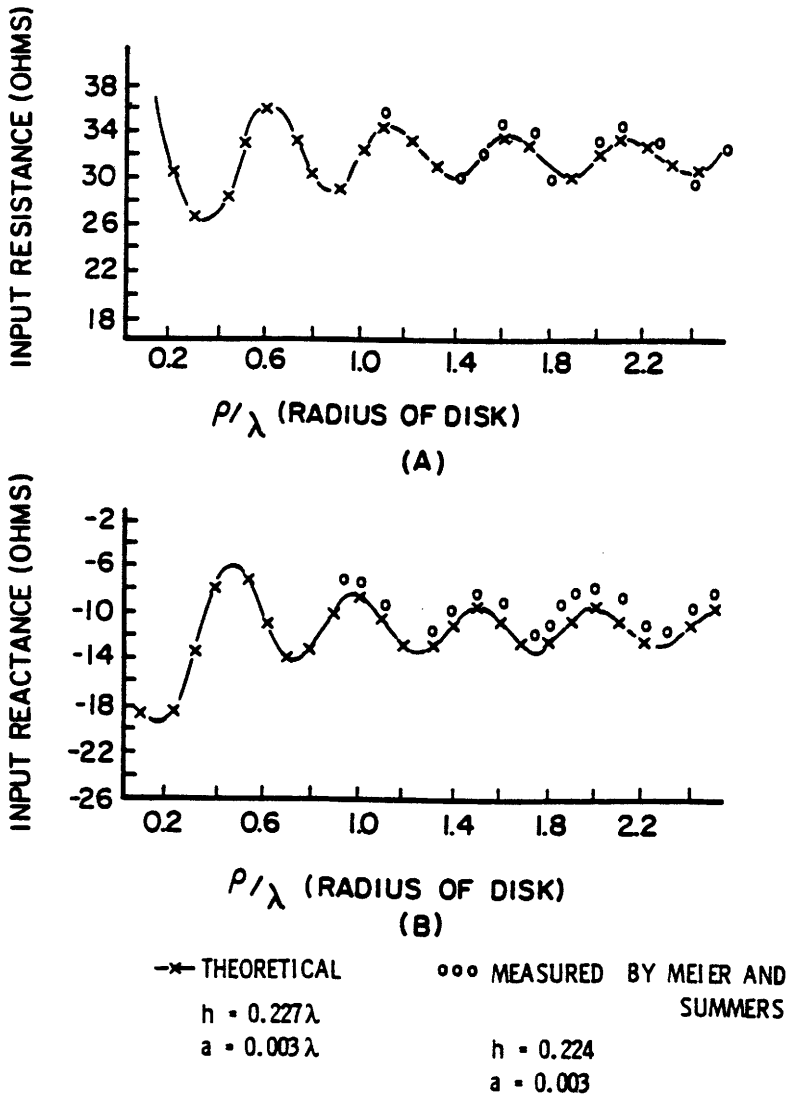

Figure 12 The input resistance and input reactance of the monopole.

V. CONCLUSION

The hybrid theory of diffraction is extended from the pure scattering case to one in which the source is near or on the scattering body. As a specific example problem we choose a monopole on a circular disk. The input impedance problem is included in the formulation by using the value of the input impedance when the antenna is on an infinite ground plane and then calculating the change in the input impedance due to the non-infinite nature of the ground plane.

While we find the hybrid theory of diffraction useful and not to require a lengthy computer code to handle the problem treated in this paper, we observe that generally the hybrid theory of diffraction is more easily applied to scattering problems such as calculating the radar cross section. For problems where the source (antenna) is located on or near the scattering body, the hybrid MM-GTD technique [10-14] is a more direct method of solution provided the required diffraction coefficients are available. If the required diffraction coefficients are not available, then the method of this paper provides an alternative approach that can treat more general geometries [17].

VI. ACKNOWLEDGEMENT

Professor Li wishes to gratefully acknowledge Professor C.T. Tai of the University of Michigan and Professor R.G. Kouyoumjian of the Ohio State University for their helpful suggestion. Appreciation is also extended to Professor Anthony Evers and Mr. Richard Zeh for their help in computer techniques.

REFERENCES

1. T.J. Kim and G.A. Thiele, "A Hybrid Diffraction Technique - General Theory and Applications, " IEEE Trans. on Antennas and Propagation, Vol. AP-30, No. 5, Sept. 1982, pp. 888-897.

2. T.J. Kim and G.A. Thiele, "A Hybrid Method Which Combines a Moment Method Current with an Asymptotic Current," The Ohio State University ElectroScience Laboratory, Dept. of Electrical Engineering, Columbus, Ohio, Technical Report 711353-2, Dec. 1980.

3. R. Mittra (Editor), Computer Techniques for Electromagnetics, Pergamon 1973, reprinted by Hemisphere Publishing 1987, Chapter 4 by A.J. Poggio and E.K. Miller, "Integral Equation Solution of Three-Dimensional Scattering Problems, " p. 167 (4.14), p. 182.

4. A. Leitnet and R.D. Spence, "Effect of a Circular Ground Plane on Antenna Radiation, " Journal of Applied Physics, Vol. 21, pp. 1001-1006, Oct. 1950.

5. Carlton H. Walter, Traveling Wave Antennas, Dover Publications Inc., N.Y., 1970, pp. 34-37, reprinted by Peninsula Publishing, Los Altos, CA, 1990.

6. James E. Storer, "The Impedance of an Antenna Over Large Circular Screens," Journal of Applied Physics, Vol. 22, No. 8, pp. 1058-1066, Aug. 1951.

7. Harry E. Green, "Radiation from a Monopole Excited Cone," IEEE Trans. Antennas and Propagation, Vol. AP-17, No. 6, pp. 707-715, Nov. 1969.

8. Harry E. Green, "Impedance of a Monopole on the Base of a large Cone," IEEE Trans. on Antennas and Propagation, Vol. AP-17, No. 6, pp. 701-706, Nov. 1969.

9. W.L. Stutzman and G.A. Thiele, Antenna Theory and Design, John Wiley & Sons, N.Y., 1981, p. 506.

10. G.A. Thiele and T.H. Newhouse, "A Hybrid Technique for Combining Moment Methods with the Geometrical Theory of Diffraction," IEEE Trans. on Antennas and Propagation, Vol. AP-23, No. 1, Jan. 1975, pp. 62-69.

11. E.P. Ekelman and G.A. Thiele, "A Hybrid MM-GTD Technique for Combining the Moment Method Treatment of Wire Antennas with the GTD for Curved Surface, " IEEE Trans. on Antennas and Propagation, Vol. AP-28, No. 6, Nov. 1980, pp. 831-839.

12. G.A. Thiele and G.K. Chan, "Application of the Hybrid Technique to Time Domain Problems," IEEE Trans. on Electromagnetic Compatibility, Vol. EMC-20, No. 1, Feb. 1978, and IEEE Trans. Antennas Propagat., (Joint Issue) Vol. AP-26, Jan. 1978, pp.151-155.

13. L.W. Henderson and G.A. Thiele, "A Hybrid MM-GTD Technique for the Treatment of Wire Antennas Near a Curved Surface," Radio Science, (Nov/Dec 1981), 16, pp.1125-1120, also see Digest of the 1980 International U.R.S.I. Electromagnetic Wave Symposium, Munich, pp. 314A/1-4.

14. S.A. Davidson and G.A. Thiele, "A Hybrid Method of Moments - GTD Technique for Computing Electromagnetic Coupling Between Two Monopole Antennas on a Large Cylindrical Surface," IEEE Transaction on Electromagnetic Compatibility, Vol. EMC-26, No. 2, May 1984, see also Proceedings of the 1981 Electromagnetics Compatibility Symposium, Zurich, pp. 277-282.

15. G.L. James, Geometrical Theory of Diffraction for Electromagnetic Waves, Peter Peregrinus Ltd., England, 1976, p. 11.

16. A.S. Meier and W.P. Summers, "Measured Impedance of Vertical Antennas Over Finite Ground Planes," Proc. IRE, vol. 37, pp. 609-616, June 1949.

17. G.A. Thiele, "Overview of Selected Hybrid Methods in Radiating System Analysis," Proc. of the IEEE, Vol., 79, No. 11, Nov. 1991 (to appear), invited.